On the Choice of Optimal Methodology for Calculation of ^{13}C and ^{1}H NMR Isotropic Chemical Shifts in Cagelike Systems. Case Studies of Adamantane, 2-Adamantanone, and 2,4-Methano-2,4-dehydroadamantane

Dražen Vikić-Topić*,† and Ljupčo Pejov‡

Ruđer Bošković Institute, NMR Center, P.O. Box 180, 10002 Zagreb, Croatia, and Institute of Chemistry, Faculty of Natural Sciences and Mathematics, Cyril and Methodius University, P.O. Box 162, 91001 Skopje, Macedonia

Received April 28, 2001

The ^{13}C and ^{1}H isotropic chemical shift values computed at HF, BLYP, B3LYP, and MPW1PW91/6-311+G-(2*d*,*p*) levels of theory, for the BLYP and B3LYP/6-31G(*d*,*p*) optimized geometries of adamantane, 2-adamantanone, and 2,4-methano-2,4-dehydroadamantane ([3.1.1] propellane) are reported and compared with the experimental data. Except for the "inverted" carbon atoms and some of their nearest neighbors, the HF values are superior over the DFT ones, when the isotropic shifts with respect to TMS are in question. However, in case of the *relative shifts* computed with respect to the most deshielded center *within* the molecule, the DFT methods yield significantly better agreement with the experimental data than the HF method, the hybrid DFT methods being superior over "pure" DFT ones. The most probable reason for these findings may be the cancellation of errors arising from the inappropriate description of the paramagnetic contributions to the overall shielding tensor within the Kohn−Sham approach when an internal standard (within a molecule) is chosen, instead of an external one. Almost excellent linear correlation was found between the calculated and experimental *relative shift* values, which is significantly superior at DFT levels than at HF level, further proving the more systematical nature of errors in predicting the second-order magnetic response properties at DFT levels of theory. Among all DFT methods employed, the MPW1PW91 showed the best performance, in line with the significantly improved long-range behavior of this functional, as compared to the B3LYP one.

1. INTRODUCTION

It is of certain interest in various areas of chemical physics to be able to accurately predict the molecular *response properties* to external fields. This statement is especially important when one considers the second-order *magnetic response* properties. Magnetic resonance based techniques have become of substantial importance in chemistry and biochemistry. An illustrative example is that the computed ^{13}C chemical shifts may be firmly used as an aid in identification of reactive ionic species.[1−3] On the other hand, the prediction of environmental dependence of the chemical shifts in case of amino acid carbon atoms might be very helpful in elucidation of three-dimensional protein structures.[4−6]

In due course, the quantities of primary interest are the nuclear magnetic shielding tensors.[7] These tensors are defined as mixed second derivatives of the molecular energy (E) with respect to magnetic moment of the Xth nucleus ($\vec{m}_X$) and external magnetic field ($\vec{B}$):

$$\sigma_X^{\alpha\beta} = \frac{\partial^2 E}{\partial B^\alpha \partial m_X^\beta}$$

The Greek superscripts in the last equation denote the corresponding vector or tensor components.

Although it has been long recognized that prediction of the second-order magnetic response properties from the first principles employing *finite basis sets* requires a gauge-independent algorithm[8−12] and the first such algorithm due to Ditchfield[10] appeared almost four decades ago, chemically reasonable predictions of NMR properties for molecular systems, especially of moderate size, have not become possible until recently. The mentioned methodology (known under the acronym GIAO−gauge independent atomic orbitals) is based on the achievement of gauge-invariance using field-dependent basis functions.[10−12] The efficient implementation of this method for routine ab initio calculations was based on techniques borrowed from analytic derivative methodologies[11,12] used in the works of Pulay and collaborators. Efficient alternative to the GIAO procedure is the CSGT (continuous set of gauge transformations) algorithm[13−15] due to Keith and Bader (and its variant known under the acronym IGAIM−individual gauge for atoms in molecules[13−15]). The nuclear magnetic shielding tensor, within this methodology, is expressed through the induced first-order electronic current density. An accurate calculation of the last quantity by performing a gauge transformation for each point in space leads to gauge-invariant values of the shielding tensors. It has been shown that both methodologies are very useful, although it seems that the GIAO procedure is somewhat superior since it exhibits a faster convergence of the calculated properties upon extension of the basis set used.[8,16−20]

* Corresponding author phone: (3851) 4680-085. Fax: (3851) 4680-084. E-mail: vikic@faust.irb.hr.
† Ruđer Bošković Institute.
‡ Cyril and Methodius University.

10.1021/ci010042m CCC: $20.00
Published on Web 10/31/2001

Other methodologies, such as IGLO[21,22] (individual gauge for localized orbitals) and LORG[23,24] (localized orbital/local origin), etc., have also been proposed, and their performances have been tested on a wide variety of molecular systems.[25−28] However, taking into account the computational cost and the effectiveness of calculation, the GIAO and CSGT methods seem to be preferable from many aspects, at least at the present state of this subject.

The importance of studying the performances of various methods for achievement of gauge invariance, especially with respect to inclusion of the dynamical electron correlation effects[29] and to the basis set size[8] from methodological aspect, is beyond any doubt. A number of studies of this type have been published,[16,30−39] although it does not seem that a definitive conclusion on the optimal choice of computational methodology has been reached. This especially refers to the problem of inclusion of dynamical electron correlation effects into the ab initio calculations of the second-order magnetic response properties. GIAO-MBPT and CC methodologies have been proposed[40−43] and successfully applied, but they are computationally demanding for even modest size molecules, which are of interest for organic chemists. Density functional theory (DFT)-based methodologies,[44,45] on the other hand, offer an efficient alternative to the conventional correlated methods, due to their significantly lower computational cost.

All DFT methods are in fact based on the *Hohenberg−Kohn theorem*,[46] which states that the electronic energy of a given molecular system is a definite functional of the corresponding density.[44−47] However, the *exact form* of this functional is not explicitly known. Various types of such (exchange and correlation) functionals have been proposed[48−54] either on a more mathematical or physical basis, but almost all of them were constructed primarily focusing the attention on the *energetics* of molecular systems. However, some of the functionals (mainly the gradient corrected ones) have shown a remarkable accuracy in predicting certain other molecular properties, such as harmonic force constants,[55−57] and even the anharmonic vibrational potentials of "floppy" molecular systems.[58] It is thus of great importance to test the performances of various functionals for prediction of second-order magnetic response properties. Several systematic studies have already been devoted to this subject,[17,37] but mainly with respect to correlation between the computed *isotropic shieldings* and the measured *chemical shifts*. It seems that little attention has been paid to the question of performances of various theoretical approaches regarding the prediction of the *relative shielding values* with respect to a given center within the same molecule.

Continuing our work[59,60] on this subject, in the present paper we report a HF SCF and density functional study of isotropic ^{13}C and ^{1}H chemical shifts for three cagelike systems: adamantane and 2-adamantanone characterized by highly stiffened structures and a 2,4-methano-2,4-dehydroadamantane (a [3.1.1] propellane) system with "inverted" carbon atoms.[61,62] We have used the optimized geometries at gradient-corrected density functional levels of theory with a DZP quality basis set for both the systems of interest and the standard for calculation of the isotropic chemical shifts (TMS). The performances of various density functional methodologies and the conventional HF SCF procedure in predicting both the ^{13}C and ^{1}H isotropic chemical shifts and the *relative shifts* with respect to the most deshielded center within a given molecule were tested. Also, the efficiency of GIAO and CSGT algorithms for achieving gauge independence was tested with respect to the previously mentioned physical properties.

2. COMPUTATIONAL DETAILS

Full geometry optimizations of adamantane, 2-adamantanone, and 2,4-methano-2,4-dehydroadamantane as well as of tetramethylsilane (TMS) were performed in redundant internal coordinates with Schlegel's gradient optimization algorithm[63] (calculating the energy derivatives analytically). The geometry optimizations were performed at two gradient-corrected density functional levels of theory. Within the first approach, a combination of Becke's exchange functional[48] with the Lee−Yang−Parr correlation one[50] was employed (the methodology denoted as B-LYP), while in the second one, Becke's three-parameter adiabatic connection exchange functional[53] was used in combination with LYP (B3-LYP). The standard 6-31G(*d*,*p*) basis set of DZP quality was used for orbital expansion in solving the Kohn−Sham equations[47] for both approaches. The stationary points found on the molecular potential energy hypersurfaces were characterized by numerical harmonic vibrational analyses. The absence of imaginary frequencies (negative eigenvalues of the Hessian matrices) confirmed that the stationary points correspond to minima, instead of saddle points. Complete harmonic vibrational analyses of the mentioned species will be published elsewhere.[64]

2.1. Calculations of Isotropic Chemical Shifts. The ^{1}H and ^{13}C NMR shielding tensors for the BLYP and B3LYP/6-31G(*d*,*p*) optimized geometries of the mentioned molecules were calculated using two methodologies for achievement of gauge independence: Gauge Independent Atomic Orbitals (GIAO) method and Continuous Set of Gauge Transformations (CSGT) methodology (for a more thorough description of these methods, see the following chapter). The Individual Gauge for Atoms in Molecules (IGAIM) approach showed in our previous works to give results which are rather close to the CSGT ones, so we only relied on the later in the present study. These calculations were performed at various theoretical levels, both with and without an inclusion of the dynamical electron correlation effects using a TZP quality basis set 6-311+G(2*d*,*p*) for orbital expansion. This basis is augmented with a diffuse *sp* shell and two sets of *d* polarization functions on carbons and oxygens and a set of *p* polarization functions on hydrogen atoms. Both standard Hartree−Fock (HF/6-311+G(2*d*,*p*)) as well as BLYP/6-311+G(2*d*,*p*), B3LYP/6-311+G(2*d*,*p*), and the MPW1PW91/6-311+G(2*d*,*p*) levels of theory were employed. The MPW1PW91 methodology is based on a combination of the Perdew−Wang 1991 exchange functional as modified by Adamo and Barone, with the Perdew and Wang's 1991 gradient-corrected correlation functional.[54] In all density functional calculations, the fine (75, 302) grid was used for numerical integration.[44,45] Note that while the BLYP methodology is nonhybrid (it includes no HF exchange)—i.e. it is a "pure" DFT method, while the B3LYP and MPW1PW91 ones contain an admixture of HF exchange (i.e. they are of a hybrid form).

The isotropic shielding values defined as

$$\sigma_{iso} = \frac{1}{3}(\sigma_{11} + \sigma_{22} + \sigma_{33})$$

(σ_{ii} being the principal tensor components) were used to calculate the isotropic chemical shifts δ with respect to TMS ($\delta_{iso}^{X} = \sigma_{iso}^{TMS} - \sigma_{iso}^{X}$).

It is worth noting at this point that the exchange and correlation functionals used in the present work for calculation of magnetic shielding properties *do not* include the magnetic field dependence explicitly. However, as mentioned before, they have been shown to yield rather accurate predictions of some other molecular properties. The overall success of density functional quantum chemistry in predicting other molecular properties, such as vibrational spectra,[55−58] has in fact stimulated work for further application of this methodology.

All calculations presented in this paper were carried out with the Gaussian 98 series of programs.[65]

2.2. Methods for Achievement of Gauge Invariance. Since a comparison of various methods for achievement of gauge invariance is presented in the present work, a brief description of the employed techniques is presented in this chapter.

Within the general SCF approach, the expression for the shielding tensor components for nucleus X reduces to

$$\sigma_X^{\alpha\beta} = \frac{\partial^2 E}{\partial B^\alpha \partial m_X^\beta} = \langle h^{(B^\alpha, m_X^\beta)} P \rangle + \langle h^{m_X^\beta} P^{B^\alpha} \rangle$$

where first and higher order derivatives are denoted with superscripts showing the variables with respect to which the differentiation is to be performed, while P is the density matrix. The derivatives of the Hamiltonian are given by

$$h_{\mu\nu}^{m_X^\beta} = \langle \chi_\mu | \hat{h}^{m_X^\beta} | \chi_\nu \rangle; \; h_{\mu\nu}^{(B^\alpha, m_X^\beta)} = \langle \chi_\mu | \hat{h}^{(B^\alpha, m_X^\beta)} | \chi_\nu \rangle$$

where

$$\hat{h}^{m_X^\beta} = -\frac{i}{c} \frac{[(\vec{r} - \vec{R}_X) \times \vec{\nabla}]_\beta}{|\vec{r} - \vec{R}_X|^3} \quad \text{and}$$

$$\hat{h}^{(B^\alpha, m_X^\beta)} = \frac{1}{2c^2} \frac{\vec{r}(\vec{r} - \vec{R}_X)\delta_{\alpha\beta} - \vec{r}_\alpha (\vec{r} - \vec{R}_X)_\beta}{|\vec{r} - \vec{R}_X|^3}$$

The derivative of the density matrix with respect to the magnetic field components is obtained by solving the corresponding coupled-perturbed equations.

Within the GIAO methodology, for calculation of magnetic properties, explicitly field-dependent wave functions are used of the following form

$$\chi_\mu(\vec{B}) = \exp\left[-\frac{i}{2c}(\vec{B} \times \vec{R}_\mu) \cdot \vec{r} \right] \cdot \chi_\mu(\vec{0})$$

where $\vec{R}_\mu$ is the basis function χ_μ position vector, while $\chi_\mu(\vec{0})$ denotes the (usual) field-independent function.

On the other hand, the CSGT approach is based on the expression for the shielding tensor components for nucleus X in terms of the induced first-order electronic current density $J^{(1)}(r)$:

Table 1. Experimental[61] and Optimized (BLYP and B3LYP/6-31G(*d*,*p*)) Geometry Parameters for Adamantane

parameters	exptl	BLYP/6-31G(*d*,*p*)	B3LYP/6-31G(*d*,*p*)
		Distances/Å	
C(s)-C(t)	1.540(2)	1.5558	1.5438
C(s)-H	1.112(4)	1.1052	1.0973
C(t)-H	1.112(4)	1.1048	1.0964
		Angles/deg	
C(s)-C(t)-C(s)	109.8(5)	109.35	109.32
C(t)-C(s)-C(t)	108.8(10)		
C(s)-C(t)-H			
C(t)-C(s)-H		110.08	110.05
H−C(s)-H	116.9(60)	106.77	106.83

$$\sigma_X^{\alpha\beta} = \frac{\partial^2 E}{\partial B^\alpha \partial m_X^\beta} = -\frac{1}{Bc} \int [\vec{r}_X \times J_\alpha^{(1)}(r)/r_X^3]_\beta d\vec{r}_X$$

Within this method, the gauge-invariance is achieved by accurate calculation of the induced first-order electronic current density, performing a gauge transformation for each point in space.

3. EXPERIMENTAL NMR MEASUREMENTS

The NMR data of adamantane and 2-adamantanone are available in the literature,[66] but we have remeasured the ^{1}H and ^{13}C NMR spectra of these compounds with higher magnetic field spectrometer to attain greater precision.[67] The spectra were recorded with a Varian Gemini 300 spectrometer, operating at 75.46 MHz for the ^{13}C nucleus. The samples were dissolved in $CDCl_3$ and measured at 20 °C in 5 mm NMR tubes. Concentrations of samples were 0.1 M for ^{1}H and 0.2 M for ^{13}C measurements. Chemical shifts (ppm) were referred to TMS as internal standard. The following measurement techniques were used: standard ^{1}H, ^{13}C broadband proton decoupling, ^{13}C gated decoupling, COSY, and HETCOR. For proton decoupling the Waltz-16 modulation was applied. Digital resolution was 0.3 Hz per point in ^{1}H and 0.5 Hz per point in ^{13}C NMR one-dimensional spectra. The COSY spectra were recorded in the magnitude mode with 1024 points in F2 dimension and 256 increments in F1 dimension, zero-filled to 1024 points. Increments were measured with 16 scans, 4500 Hz spectral width, and a relaxation delay of 1 s. The corresponding digital resolution was 8.9 Hz/point and 17.6 Hz/point in F2 and F1 dimensions, respectively. The HETCOR spectra were recorded with 2048 points in F2 dimension and 256 increments in F1 dimension The latter was zero-filled to 512 points. Increments were recorded by 64 scans with relaxation delay of 0.8 s. Spectral widths were 19 000 Hz in F2 and 4500 Hz in F1 dimensions, giving digital resolution of 18.6 Hz/point and 17.6 Hz/point, respectively.

4. RESULTS AND DISCUSSION

The optimized geometry parameters for the studied systems at BLYP and B3LYP/6-31G(*d*,*p*) levels of theory, together with the experimental electron diffraction data are presented in Tables 1−3. As can be seen, the agreement between theory and experiment is rather good. Since structural data are not available for 2,4-methano-2,4-dehydroadamantane (the [3.1.1] propellane), the optimized parameters for this system are compared with the available data

Table 2. BLYP and B3LYP/6-31G(*d*,*p*) Optimized Geometry Parameters for 2,4-Methano-2,4-dehydroadamantane Together with the Selected Experimental Data for [1.1.1] Propellane

parameters	exptl	BLYP/6-31G(*d*,*p*)	B3LYP/6-31G(*d*,*p*)
		Distances/Å	
C(1)−C(2)		1.5443	1.5329
C(2)−C(3)		1.5146	1.5005
C(2)−C(4)	1.596	1.5993	1.5660
C(2)−C(5)		1.5232	1.5095
C(5)−C(6)	1.525	1.5253	1.5150
C(6)−C(7)		1.5499	1.5374
C(7)−C(11)		1.5595	1.5471
C(11)−C(1)		1.5576	1.5460
C(1)−C(10)		1.5646	1.5524
C(1)−H	1.106	1.1032	1.0953
C(3)−H_{ax}		1.0987	1.0920
C(3)−H_{eq}		1.0936	1.0864
C(5)−H	1.106	1.1023	1.0947
C(6)−H		1.1045	1.0969
C(7)−H		1.1038	1.0970
C(8)−H_{eq}		1.1042	1.0974
C(8)−H_{ax}		1.1040	1.0971
C(10)−H_{eq}		1.1016	1.0942
C(10)−H_{ax}		1.1044	1.0979
		Angles/deg	
C(2)−C(3)-C(4)		63.7	62.9
C(2)−C(5)-C(4)		63.3	62.5
C(2)−C(5)-C(6)		118.6	118.4
C(1)−C(10)-C(9)		100.6	100.7
C(11)−C(7)-C(8)		111.4	111.4

Table 3. Experimental and Optimized Geometry Parameters for 2-Adamantanone at BLYP and B3LYP/6-31G(*d*,*p*) Levels of Theory

parameter	exptl	BLYP/6-31G(*d*,*p*)	B3LYP/6-31G(*d*,*p*)
		Distances/Å	
r(C═O)	1.240	1.229	1.217
r(C1−C2)	1.540	1.540	1.527
		Angles/deg	
α (C2C1C2)	109.5	112.4	112.6
α (C1C2C3)	109.5	108.4	108.3
α (C2C3C4)	109.5	109.8	109.8
α (C1C2H)	109.5	108.4	108.3
α (OC1C2)		123.8	123.7

Figure 1. Molecular structure of adamantane.

for [1.1.1] propellane (Table 2). The agreement is again pretty good. The structures of adamantane, 2-adamantanone, and 2,4-methano-2,4-dehydroadamantane, together with the atomic numbering for the last two systems are shown in Figures 1−3, respectively.

Accurate molecular geometries are, of course, essential for reliable calculations of magnetic properties. Although it is sometimes convenient to use even the available experimental geometry, to have consistent results for all of the studied systems, we relied on the DFT optimized geometries. Since the agreement with the available experimental data is rather good, and, further, it has been recognized that the derivatives of the form $(\partial\sigma/\partial q_i)$ (q_i being a geometry parameter) are rather small for both ^{13}C and ^{1}H shieldings,[68] we regard the adopted approach as fully appropriate.

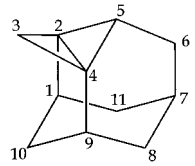

Figure 2. Molecular structure and atomic numbering for [3.1.1] propellane.

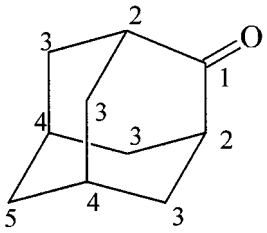

Figure 3. Molecular structure and atomic numbering for 2-adamantanone.

Table 4. Theoretical and Experimental ^{13}C and ^{1}H Isotropic Chemical Shifts (with Respect to TMS, All Values in ppm) for Adamantane[b]

B3LYP/6-31G(*d*,*p*) optimized geometry				
	C(t)[a]		C(s)[a]	
method	CSGT	GIAO	CSGT	GIAO
MPW1PW91	33.43	33.64	40.76	40.51
B3LYP	35.51	36.00	42.58	42.63
BLYP	38.13	38.86	44.80	45.01
HF	28.04	27.92	35.86	35.50
experimental	28.16		37.58	
	H(t)[a]		H(s)[a]	
method	CSGT	GIAO	CSGT	GIAO
MPW1PW91	1.68	1.84	1.77	1.75
B3LYP	1.70	1.86	1.81	1.80
BLYP	1.80	1.98	1.94	1.94
HF	2.02	1.47	2.16	1.44
experimental	1.87		1.75	
BLYP/6-31G(*d*,*p*) optimized geometry				
	C(t)[a]		C(s)[a]	
method	CSGT	GIAO	CSGT	GIAO
MPW1PW91	34.38	34.52	40.92	40.66
B3LYP	36.49	36.92	42.74	42.79
BLYP	39.11	39.75	44.94	45.14
HF	28.90	28.81	36.01	35.69
experimental	28.16		37.58	
	H(t)[a]		H(s)[a]	
method	CSGT	GIAO	CSGT	GIAO
MPW1PW91	1.67	1.84	1.75	1.73
B3LYP	1.69	1.86	1.78	1.78
BLYP	1.79	1.98	1.91	1.92
HF	1.36	1.47	1.44	1.43
experimental	1.87		1.75	

[a] "s" and "t" denote a secondary and tertiary carbon or hydrogen atom correspondingly. [b] All calculations were performed with the 6-311+G(2*d*,*p*) basis set.

The calculated isotropic ^{13}C and ^{1}H chemical shifts (with respect to TMS) for adamantane, 2-adamantanone, and 2,4-methano-2,4-dehydroadamantane at HF/6-311+G(2*d*,*p*) as well as at density functional BLYP, B3LYP, and MPW1-

Table 5. Theoretical ^{13}C and ^{1}H and Experimental ^{13}C Isotropic Chemical Shifts (with Respect to TMS, All Values in ppm) for 2,4-Methano-2,4-dehydroadamantane[a]

		CSGT				GIAO			
atom	exp.	MPW1PW91	B3LYP	BLYP	HF	MPW1PW91	B3LYP	BLYP	HF
C1	35.0	39.48	41.03	43.27	33.12	39.66	41.5	43.87	33.33
C2	24.2	24.69	25.37	27.45	14.33	25.89	26.82	29.07	15.34
C3	40.9	40.95	41.12	41.02	39.08	41.61	42.06	42.12	39.45
C4	24.2	24.69	25.37	27.45	14.33	25.89	26.82	29.07	15.34
C5	64.4	65.66	66.55	67.66	60.07	66.43	67.69	69.04	60.53
C6	30.8	33.39	34.81	36.55	29.51	33.12	34.83	36.63	29.5
C7	26.6	31.56	33.44	35.76	26.42	31.71	33.83	36.27	26.48
C8	34.2	37.17	38.81	40.73	32.95	36.96	38.88	40.9	32.83
C9	44.0	39.48	41.03	43.27	33.12	39.66	41.5	43.87	33.33
C10	50.1	51.81	52.88	54.22	46.65	52.07	53.36	54.76	47.01
C11	34.2	37.17	38.81	40.73	32.95	36.96	38.88	40.9	32.83
H(C1)		2.21	2.23	2.33	1.90	2.38	2.40	2.51	2.054
H_{eq}(C3)		1.82	1.80	1.82	1.72	2.02	2.02	2.05	1.934
H_{ax}(C3)		0.76	0.73	0.71	0.71	0.99	0.97	0.96	0.944
H(C5)		2	2.00	2.08	1.71	2.17	2.19	2.29	1.864
H′(C6)		1.82	1.86	1.96	1.59	1.94	1.99	2.10	1.694
H″(C6)		1.82	1.86	1.96	1.59	1.94	1.99	2.10	1.694
H(C7)		1.59	1.60	1.69	1.26	1.79	1.80	1.90	1.444
H_{eq}(C8)		1.51	1.54	1.63	1.28	1.60	1.64	1.74	1.354
H_{ax}(C8)		1.48	1.49	1.59	1.21	1.53	1.56	1.66	1.274
H(C9)		2.21	2.23	2.33	1.90	2.38	2.40	2.51	2.054
H_{eq}(C10)		2.3	2.30	2.42	1.84	2.48	2.49	2.62	2.014
H_{ax}(C10)		1.71	1.71	1.82	1.37	1.78	1.79	1.92	1.454
H_{eq}(C11)		1.48	1.49	1.59	1.21	1.53	1.56	1.66	1.274
H_{ax}(C11)		1.51	1.54	1.63	1.28	1.60	1.64	1.74	1.354

[a] All calculations with the 6-311+G(2*d*,*p*) basis set, for B3LYP/6-31G(*d*,*p*) optimized geometry.

Table 6. Theoretical ^{13}C and ^{1}H and Experimental ^{13}C Isotropic Chemical Shifts (with Respect to TMS, All Values in ppm) for 2,4-Methano-2,4-dehydroadamantane[a]

		CSGT				GIAO			
atom	exp.	MPW1PW91	B3LYP	BLYP	HF	MPW1PW91	B3LYP	BLYP	HF
C1	35.0	40.51	42.12	44.38	34.05	40.73	42.64	45.01	34.31
C2	24.2	27.06	27.87	29.96	16.58	28.30	29.36	31.61	17.65
C3	40.9	43.43	43.61	43.41	41.76	44.15	44.63	44.56	42.21
C4	24.2	27.06	27.87	29.96	16.58	28.30	29.36	31.61	17.65
C5	64.4	68.56	69.51	70.52	63.23	69.42	70.75	71.98	63.31
C6	30.8	33.75	35.17	36.91	29.84	33.56	35.27	37.06	29.88
C7	26.6	32.38	34.29	36.61	27.17	32.51	34.67	37.09	27.26
C8	34.2	37.45	39.1	41.01	33.2	37.26	39.18	41.18	33.12
C9	44.0	40.52	42.12	44.38	34.05	40.73	42.64	45.01	34.31
C10	50.1	53.11	54.2	55.55	47.76	53.39	54.7	56.1	48.15
C11	34.2	37.45	39.1	41.01	33.2	37.26	39.18	41.18	33.12
H(C1)		2.20	2.22	2.31	2.16	2.37	2.40	2.51	2.05
H_{eq}(C3)		1.95	1.94	1.95	1.86	2.16	2.16	2.19	2.07
H_{ax}(C3)		0.89	0.86	0.84	0.85	1.11	1.11	1.09	1.08
H(C5)		2.12	2.11	2.19	1.84	2.29	2.31	2.41	2.00
H′(C6)		1.83	1.86	1.96	1.60	1.94	2.00	2.11	1.70
H″(C6)		1.83	1.86	1.96	1.60	1.94	2.00	2.11	1.70
H(C7)		1.58	1.59	1.67	1.26	1.78	1.80	1.90	1.45
H_{eq}(C8)		1.51	1.54	1.63	1.28	1.59	1.64	1.74	1.35
H_{ax}(C8)		1.46	1.48	1.57	1.20	1.51	1.55	1.65	1.26
H(C9)		2.20	2.22	2.31	1.89	2.37	2.40	2.51	2.05
H_{eq}(C10)		2.35	2.34	2.47	1.87	2.52	2.53	2.67	2.05
H_{ax}(C10)		1.76	1.76	1.87	1.41	1.83	1.86	1.98	1.49
H_{eq}(C11)		1.46	1.48	1.57	1.20	1.51	1.55	1.65	1.26
H_{ax}(C11)		1.51	1.54	1.63	1.28	1.59	1.64	1.74	1.35

[a] All calculations with the 6-311+G(2*d*,*p*) basis set, for BLYP/6-31G(*d*,*p*) optimized geometry.

PW91/6-311+G(2*d*,*p*) levels of theory for BLYP and B3LYP/6-31G(*d*,*p*) optimized geometries (employing both GIAO and CSGT methods for achievement of gauge independence) are presented in Tables 4−8, together with the experimentally measured values.

On the other hand, in Tables 9−12, the relative ^{13}C (and ^{1}H) shift values with respect to the most deshielded atoms in the structures of adamantane, 2,4-methano-2,4-dehydroadamantane, and 2-adamantanone are given.

The following conclusions can be straightforwardly derived on the basis of presented data. Regarding the "absolute" values of the isotropic ^{13}C chemical shifts for all of the studied systems, the HF results are in almost excellent agreement with the experiment. Although in certain cases

Table 7. Theoretical Isotropic ^{13}C Chemical Shifts Computed with Respect to TMS for 2-Adamantanone Together with the Experimental Data[a]

	HF	BLYP	B3LYP	MPW1PW91	exptl
B3LYP/6-31G(*d*,*p*) Optimized Geometry					
CSGT					
C1	221.50	222.72	224.35	222.95	218.5
C2	43.42	56.44	53.33	51.31	46.7
C3	35.60	46.87	44.06	42.45	39.0
C4	27.37	37.55	34.93	32.96	27.1
C5	34.96	43.71	41.54	39.85	36.0
GIAO					
C1	221.37	223.27	224.74	222.90	218.5
C2	43.85	56.83	53.72	51.41	46.7
C3	35.48	47.08	44.16	42.25	39.0
C4	27.43	37.69	35.02	32.80	27.1
C5	34.79	43.77	41.51	39.54	36.0
BLYP/6-31G(*d*,*p*) Optimized Geometry					
CSGT					
C1	224.74	224.94	226.82	225.31	218.5
C2	44.36	57.49	54.39	52.34	46.7
C3	35.85	47.20	44.38	42.76	39.0
C4	28.20	38.50	35.87	33.88	27.1
C5	35.15	43.91	41.75	40.06	36.0
GIAO					
C1	224.74	225.61	227.33	225.38	218.5
C2	44.84	57.82	54.73	52.39	46.7
C3	35.78	47.44	44.51	42.58	39.0
C4	28.28	38.59	35.93	33.68	27.1
C5	35.02	43.98	41.74	39.76	36.0

[a] All calculations were performed with the 6-311+G(2*d*,*p*) basis set, all values in ppm.

Table 8. Theoretical Isotropic ^{1}H Chemical Shift Values Computed with Respect to TMS for 2-Adamantanone Together with the Experimental Data[a]

	HF	BLYP	B3LYP	MPW1PW91	exptl
B3LYP/6-31G(*d*,*p*) Optimized Geometry					
CSGT					
H(C2)	2.02	2.18	2.16	2.17	2.5
H(C3)eq.	1.59	2.11	1.97	1.94	2.1
H(C3)ax.	1.49	2.02	1.88	1.86	2.0
H(C4)	1.45	1.80	1.73	1.71	1.9
H(C5)	1.58	2.01	1.90	1.88	2.0
GIAO					
H(C2)	2.27	2.45	2.41	2.42	2.5
H(C3)eq.	1.64	2.22	2.05	2.01	2.1
H(C3)ax.	1.60	2.17	2.02	1.98	2.0
H(C4)	1.60	1.98	1.90	1.87	1.9
H(C5)	1.62	2.08	1.96	1.92	2.0
BLYP/6-31G(*d*,*p*) Optimized Geometry					
CSGT					
H(C2)	2.05	2.20	2.18	2.19	2.5
H(C3)eq.	1.58	2.09	1.95	1.93	2.1
H(C3)ax.	1.49	2.00	1.87	1.85	2.0
H(C4)	1.45	1.79	1.72	1.71	1.9
H(C5)	1.57	1.98	1.88	1.86	2.0
GIAO					
H(C2)	2.32	2.47	2.44	2.01	2.5
H(C3)eq.	1.64	2.21	2.04	1.57	2.1
H(C3)ax.	1.59	2.16	2.01	1.54	2.0
H(C4)	1.61	1.98	1.90	1.44	1.9
H(C5)	1.61	2.06	1.94	1.47	2.0

[a] All calculations were performed with the 6-311+G(2*d*,*p*) basis set, all values in ppm.

the CSGT values are slightly superior over the GIAO, these two methods yield values that are rather close, confirming that the convergence with respect to basis set size has been achieved. Among all of the density functional methods, the

Table 9. Theoretical and Experimental $\delta_{iso}(C(s)) - \delta_{iso}(C(t))$ and $\delta_{iso}(H(t)) - \delta_{iso}(H(s))$ Values (in ppm) for Adamantane[a]

B3LYP/6-31G(*d*,*p*) Optimized Geometry		
	$\delta_{iso}(C(s)) - \delta_{iso}(C(t))$	
method	CSGT	GIAO
MPW1PW91	7.33	6.87
B3LYP	7.07	6.63
BLYP	6.67	6.15
HF	7.82	7.58
experimental	9.42	
	$\delta_{iso}(H(t)) - \delta_{iso}(H(s))$	
method	CSGT	GIAO
MPW1PW91	−0.09	0.09
B3LYP	−0.11	0.06
BLYP	−0.14	0.04
HF	−0.14	0.03
experimental	0.12	
BLYP/6-31G(*d*,*p*) Optimized Geometry		
	$\delta_{iso}(C(s)) - \delta_{iso}(C(t))$	
method	CSGT	GIAO
MPW1PW91	6.54	6.14
B3LYP	6.25	5.87
BLYP	5.83	5.39
HF	7.11	6.88
experimental	9.42	
	$\delta_{iso}(H(t)) - \delta_{iso}(H(s))$	
method	CSGT	GIAO
MPW1PW91	−0.08	0.11
B3LYP	−0.09	0.08
BLYP	−0.12	0.06
HF	−0.08	0.04
experimental	0.12	

[a] All calculations performed with the 6-311G(d,p) basis set.

MPW1PW91 performs best with respect to prediction of the isotropic ^{13}C chemical shifts, in line with the recent findings of Wiberg.[37] (We outline a rigorous physical basis for this finding further in this chapter.) However, the MPW1PW91 combination of functionals is still inferior with respect to HF. It is worth noting that although being principally superior, the standard HF methodology does not yield a *systematically* better agreement with the experiment as compared to the DFT-based methodologies. This is reflected in the values of the RMS deviations of the computed absolute ^{13}C shifts from the experimental data (available from the atuthors upon request), which are in some cases larger than the values obtained with DFT methods, although it is evident that the *overall* agreement with the experiment is obviously better at the HF level. For certain carbon centers (e.g. for the inverted carbon atoms within [3.1.1]propellane, and their close neighbors—see Tables 5 and 6), the HF SCF methodology yields significantly inferior values with respect to DFT ones.

With respect to the geometry optimization method, generally speaking, the isotropic chemical shifts calculated for the B3LYP/6-31G(*d*,*p*) optimized geometries are systematically better than those for the BLYP/6-31G(*d*,*p*) ones, regardless on the level of theory and the method for achievement of gauge invariance employed.

Regarding the absolute values of the ^{1}H isotropic shifts, it is very interesting that the DFT methods are superior over

Table 10. Theoretical and Experimental Relative ^{13}C Isotropic Chemical Shifts (with Respect to the Most Deshielded C5 Center within the Molecule) for 2,4-Methano-2,4-dehydroadamantane[a]

		CSGT				GIAO			
atom	exp.	MPW1PW91	B3LYP	BLYP	HF	MPW1PW91	B3LYP	BLYP	HF
				B3LYP/6-31G(*d*,*p*) Optimized Geometry					
C1	29.4	26.18	25.52	24.39	26.95	26.77	26.19	25.17	27.2
C2	40.2	40.97	41.18	40.21	45.74	40.54	40.87	39.97	45.19
C3	23.5	24.71	25.43	26.64	20.99	24.82	25.63	26.92	21.08
C4	40.2	40.97	41.18	40.21	45.74	40.54	40.87	39.97	45.19
C5	0	0	0	0	0	0	0	0	0
C6	33.6	32.27	31.74	31.11	30.56	33.31	32.86	32.41	31.03
C7	37.8	34.10	33.11	31.90	33.65	34.72	33.86	32.77	34.05
C8	30.2	28.49	27.74	26.93	27.12	29.47	28.81	28.14	27.70
C9	20.4	26.18	25.52	24.39	26.95	26.77	26.19	25.17	27.20
C10	14.3	13.85	13.67	13.44	13.42	14.36	14.33	14.28	13.52
C11	30.2	28.49	27.74	26.93	27.12	29.47	28.81	28.14	27.70
				BLYP/6-31G(*d*,*p*) Optimized Geometry					
atom	exp.	MPW1PW91	B3LYP	BLYP	HF	MPW1PW91	B3LYP	BLYP	HF
C1	29.4	28.05	27.39	26.14	29.18	28.69	28.11	26.97	29
C2	40.2	41.50	41.64	40.56	46.65	41.12	41.39	40.37	45.66
C3	23.5	25.13	25.90	27.11	21.47	25.27	26.12	27.42	21.10
C4	40.2	41.50	41.64	40.56	46.65	41.12	41.39	40.37	45.66
C5	0	0	0	0	0	0	0	0	0
C6	33.6	34.81	34.34	33.61	33.39	35.86	35.48	34.92	33.43
C7	37.8	36.18	35.22	33.91	36.06	36.91	36.08	34.89	36.05
C8	30.2	31.11	30.41	29.51	30.03	32.16	31.57	30.80	30.19
C9	20.4	28.04	27.39	26.14	29.18	28.69	28.11	26.97	29
C10	14.3	15.45	15.31	14.97	15.47	16.03	16.05	15.88	15.16
C11	30.2	31.11	30.41	29.51	30.03	32.16	31.57	30.80	30.19

[a] All calculations with the 6-311+G(2*d*,*p*) basis set, all values in ppm.

Table 11. Theoretical Relative Isotropic ^{13}C Chemical Shift Values Computed with Respect to the Most Deshielded Internal Center (Carbonyl C) for 2-Adamantanone and Corresponding Differences of Experimental Isotropic Chemical Shift Values[a]

	HF	BLYP	B3LYP	MPW1PW91	exptl
			B3LYP/6-31G(*d*,*p*) Optimized Geometry		
CSGT					
C1	0.00	0.00	0.00	0.00	0.00
C2	178.08	166.29	171.02	171.64	171.8
C3	185.90	175.86	180.30	180.50	179.5
C4	194.14	185.17	189.42	189.99	191.4
C5	186.54	179.01	182.82	183.10	182.5
GIAO					
C1	0.00	0.00	0.00	0.00	0.00
C2	177.52	166.44	171.03	171.49	171.8
C3	185.89	176.19	180.58	180.65	179.5
C4	193.94	185.58	189.72	190.10	191.4
C5	186.58	179.50	183.24	183.36	182.5
			BLYP/6-31G(*d*,*p*) Optimized Geometry		
CSGT					
C1	0.00	0.00	0.00	0.00	0.00
C2	180.38	167.45	172.43	172.98	171.8
C3	188.89	177.75	182.44	182.56	179.5
C4	196.54	186.44	190.95	191.44	191.4
C5	189.58	181.04	185.07	185.26	182.5
GIAO					
C1	0.00	0.00	0.00	0.00	0.00
C2	179.90	167.79	172.60	172.99	171.8
C3	188.96	178.17	182.82	182.79	179.5
C4	196.45	187.02	191.40	191.70	191.4
C5	189.72	181.63	185.60	185.62	182.5

[a] All calculations were performed with the 6-311+G(2*d*,*p*) basis set, all values in ppm.

Table 12. Theoretical Relative Isotropic ^{1}H Chemical Shift Values Computed with Respect to the Most Deshielded Internal Center (H2) for 2-Adamantanone and Corresponding Differences of Experimental Isotropic Chemical Shift Values[a]

	HF	BLYP	B3LYP	MPW1PW91	exptl
			B3LYP/6-31G(*d*,*p*) Optimized Geometry		
CSGT					
H(C2)	0	0	0	0	0
H(C3)eq.	0.43	0.07	0.19	0.23	0.4
H(C3)ax.	0.52	0.17	0.27	0.31	0.5
H(C4)	0.57	0.39	0.43	0.46	0.6
H(C5)	0.43	0.17	0.25	0.29	0.5
GIAO					
H(C2)	0.00	0.00	0.00	0.00	0
H(C3)eq.	0.63	0.23	0.36	0.41	0.4
H(C3)ax.	0.68	0.28	0.40	0.44	0.5
H(C4)	0.67	0.47	0.52	0.55	0.6
H(C5)	0.65	0.37	0.45	0.50	0.5
			BLYP/6-31G(*d*,*p*) Optimized Geometry		
CSGT					
H(C2)	0.00	0.00	0.00	0.00	0
H(C3)eq.	0.47	0.11	0.23	0.27	0.4
H(C3)ax.	0.57	0.20	0.31	0.35	0.5
H(C4)	0.61	0.41	0.46	0.49	0.6
H(C5)	0.48	0.22	0.30	0.33	0.5
GIAO					
H(C2)	0.00	0.00	0.00	0.00	0
H(C3)eq.	0.68	0.26	0.40	0.45	0.4
H(C3)ax.	0.72	0.31	0.43	0.48	0.5
H(C4)	0.71	0.49	0.54	0.57	0.6
H(C5)	0.71	0.41	0.50	0.54	0.5

[a] All calculations were performed with the 6-311+G(2*d*,*p*) basis set, all values in ppm).

the HF if compared with available experimental data. Such conclusion might be very valuable for adoption of a general strategy for calculation of ^{1}H isotropic chemical shift values. It has been well recognized that the calculations of proton shifts need to be at least an order of magnitude more accurate (in an absolute sense) than the ^{13}C ones, to be equally useful.

This is so because the typical ^{1}H chemical shift values range from 0 to 12 ppm, while ^{13}C ones range roughly from 0 to 220 ppm. However, in the present case, at least a part of this excellent agreement with the experimental results might be due to the somewhat more pronounced deviations of the DFT optimized C−H distances compared to the experimental ones, than of the C−C ones, leading to cancellation of various errors.

The question now arises why the density functional theory methods generally yield worse agreement with the experimental data, at least for the ^{13}C isotropic chemical shifts (with respect to TMS), and is it possible to improve the performances of DFT methods in this respect? First of all, it has been firmly elaborated that the currently available exchange and correlation functionals are not *a priori* expected to yield accurate magnetic properties of molecular systems, due to several reasons. Namely, the developed functionals have been parametrized for calculation of energetic properties and are thus expected to perform best for calculations of such properties.[36,44,45] Further, and certainly more important, is the following consideration. The paramagnetic contribution to the overall shielding tensor component within the DFT generalized gradient approximation (GGA) is given by[36]

$$\sigma_{\mathrm{p}}^{\mathrm{X}\alpha\beta} = -\sum_{j=1}^{n}\sum_{b=n+1}^{m} \frac{\langle b|l^{\alpha}|j\rangle\langle j|l_{\mathrm{X}}^{\beta}\, r_{\mathrm{X}}^{-3}|b\rangle + \langle b|l_{\mathrm{X}}^{\alpha}\, r_{\mathrm{X}}^{-3}|j\rangle\langle j|l^{\beta}|b\rangle}{(\epsilon_b - \epsilon_j)}$$

(where r_X is the electron − nucleus X distance, l is the angular momentum operator, while the Greek superscripts denote vector or tensor components). Due to the underestimation of the $\epsilon_a - \epsilon_i$ energy differences (where the subscript a refers to virtual orbitals, while i refers to occupied ones), the DFT methods overestimate the paramagnetic shielding terms, which would lead to "too deshielded" centers.

As can be seen from Tables 4−8, the density functional calculations lead to exactly "too deshielded" ^{13}C centers if we compare the computed δ values with the experiment. Physically, the underestimation of the $\epsilon_a - \epsilon_i$ terms is due to the fact that the functionals that are currently in use for DFT calculations vanish too quickly to zero. This leads to wrong Kohn−Sham solutions for the virtual states, as the exchange-correlation functional has wrong behavior (being severely too shallow). Any perturbation theoretic approach based on these solutions would therefore lead to erroneous predictions. In a recent study, an attempt to overcome this weak point of the GGA approximation was presented, basing on the usage of two novel functionals—HCTH, and its asymptotically corrected variant—HCTH(AC).[36] Another efficient algorithm for improvement of these results is based on Malkin's sum-over-states density functional perturbation theory (SOS-DFPT) where level shift corrections are applied to the Kohn−Sham orbital energies.[36] The last approach was shown to lead to a substantial improvement in the calculated magnetic properties.

Is there another way that this weak point of DFT approaches could be in a sense eliminated? To further test the performances of the employed DFT and HF methodologies with respect to prediction of both ^{13}C and ^{1}H isotropic chemical shifts, we have calculated the *relative isotropic shifts* (with respect to the most deshielded centers within the studied molecules) and compared these values with the experimental data (Tables 9−12). Contrary to the previous discussion, the DFT results were found to be significantly superior over the HF ones in the present case. The performances of pure DFT approach (BLYP) are somewhat poorer than of the hybrid (B3LYP and MPW1PW91) DFT methods with respect to prediction of the relative shieldings within the molecule, as can be seen from the comparisons with the experimental data. This conclusion is a rather important one, since it implies that the density functional description of the magnetic properties of centers within a molecule (on a relative scale) is superior over the HF. Such findings may be attributed to the fact that the errors arising form the inappropriate description of virtual states within the Kohn−Sham approach in a sense cancel when the computed values are referred to a particular center *within* the same molecule, instead of to an *external* standard, such as TMS. It is important to note at this point that the MPW1PW91 DFT is the method of choice for calculation of the relative ^{13}C isotropic shift values (with respect to the most deshielded center within particular molecule).

Table 13. Parameters of Correlation Equations of the Form $[\delta_{iso}(C(5)) - \delta_{iso}(C(i))]_{theor.} = a + b \bullet [\delta_{iso}(C(5)) - \delta_{iso}(C(i))]_{exp.}$ Together with the r^2 Values for 2,4-Methano-2,4-dehydroadamantane

	method	a	b	r^2
	B3LYP/6-31G(*d*,*p*) Optimized Geometry			
CSGT	HF	3.2437	0.8856	0.9053
	BLYP	0.4701	1.0296	0.9352
	B3LYP	0.3930	1.0090	0.9457
	MPW1PW91	0.0131	1.0116	0.9550
GIAO	HF	2.7142	0.9002	0.9163
	BLYP	−0.3956	1.0383	0.9450
	B3LYP	−0.3320	1.0169	0.9536
	MPW1PW91	−0.5836	1.0181	0.9598
	BLYP/6-31G(*d*,*p*) Optimized Geometry			
CSGT	HF	1.8644	0.8780	0.9243
	BLYP	−0.8414	1.0233	0.9512
	B3LYP	−0.8167	0.9972	0.9579
	MPW1PW91	−0.9711	0.9923	0.9610
GIAO	HF	1.5929	0.8949	0.9310
	BLYP	−1.5019	1.0224	0.9535
	B3LYP	−1.3568	0.9964	0.9591
	MPW1PW91	−1.3877	0.9907	0.9592

In addition, the relative ^{13}C shift values were found to correlate almost excellently with the values computed from the experimental data, the correlation being significantly superior for the DFT methods than in the case of HF. The parameters of the correlation equations, together with the corresponding r^2 values, are given in Tables 13 and 14. Note that although the number of data points used for correlation in the case of 2-adamantanone is rather small, the range of values spanned is very large, so the excellent correlation may not be regarded as purely fortious. In Figures 4 and 5, selected theoretical relative ^{13}C shift values are plotted vs the experimental ones for [3.1.1] propellane and 2-adamantanone. The correlation lines and equations, together with the r^2 values for those particular cases, are shown as well.

Both the systematically better estimates of the relative ^{13}C and ^{1}H shielding values and the better correlation with the experimental data in the case of DFT methods (in comparison with HF) suggest that the DFT-based approaches are able to provide a systematically better description of the second-order magnetic response properties, when an *intramolecular* standard is chosen for reference. The fact that the MPW1PW91

Table 14. Parameters of Correlation Equations of the Form $[\delta_{iso}(C(1)) - \delta_{iso}(C(i))]_{theor.} = a + b \bullet [\delta_{iso}(C(1)) - \delta_{iso}(C(i))]_{exp.}$ Together with the r^2 Values for 2-Adamantanone

	method	*a*	*b*	r^2
	B3LYP/6-31G(*d*,*p*) Optimized Geometry			
CSGT	HF	−0.1728	0.9751	0.9996
	BLYP	0.0146	1.0266	0.9998
	B3LYP	−0.0463	1.0026	0.9998
	MPW1PW91	−0.056	1.0004	0.9999
GIAO	HF	−0.1582	0.9759	0.9996
	BLYP	0.0308	1.0245	0.9998
	B3LYP	−0.0291	1.0011	0.9998
	MPW1PW91	−0.0401	0.9998	0.9999
	BLYP/6-31G(*d*,*p*) Optimized Geometry			
CSGT	HF	−0.1718	0.9612	0.9995
	BLYP	0.0315	1.0174	0.9996
	B3LYP	−0.0337	0.9925	0.9997
	MPW1PW91	−0.0404	0.9908	0.9998
GIAO	HF	−0.1547	0.9616	0.9995
	BLYP	0.0445	1.0146	0.9996
	B3LYP	−0.0178	0.9903	0.9997
	MPW1PW91	−0.0315	0.9895	0.9998

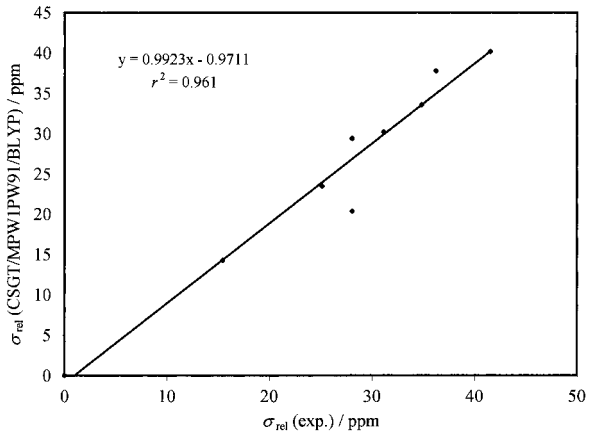

Figure 4. (a) A plot of the CSGT MPW1PW91/6-311+G(2*d*,*p*)//BLYP/6-31G(*d*,*p*) theoretical ^{13}C relative shift values vs the experimental ones for [3.1.1] propellane and (b) a plot of the CSGT HF/6-311+G(2*d*,*p*)//BLYP/6-31G(*d*,*p*) theoretical ^{13}C relative shift values vs the experimental ones for [3.1.1] propellane.

approach is superior over both BLYP and B3LYP ones from any aspect is further in line with the assumptions outlined previously, that the errors arising from the inappropriate description of virtual states in a sense cancel when choosing an internal standard for a reference. The MPW1PW91 combination of functionals was designed exactly with the main aim to improve the long-range behavior and thus the

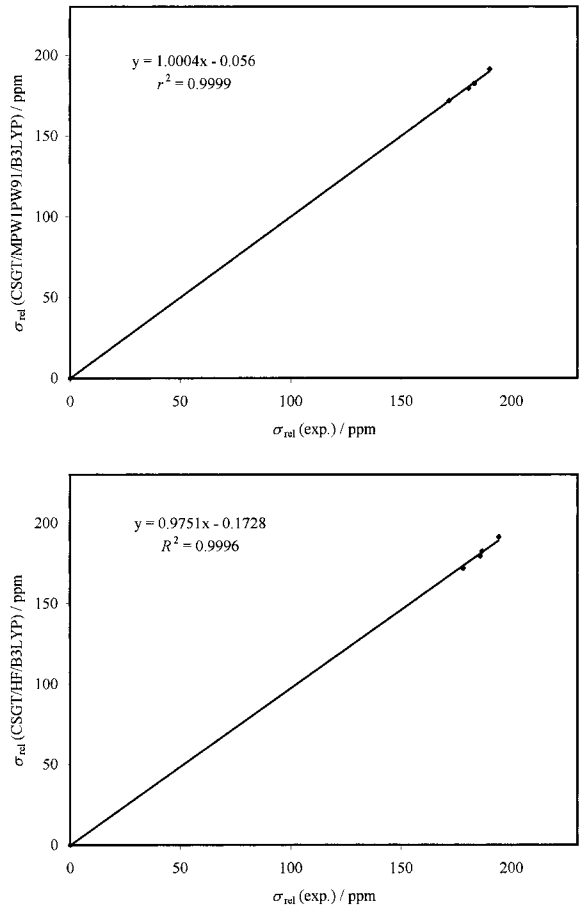

Figure 5. (a) A plot of the CSGT MPW1PW91/6-311+G(2*d*,*p*)//B3LYP/6-31G(*d*,*p*) theoretical ^{13}C relative shift values vs the experimental ones for 2-adamantanone and (b) a plot of the CSGT HF/6-311+G(2*d*,*p*)//B3LYP/6-31G(*d*,*p*) theoretical ^{13}C relative shift values vs the experimental ones for 2-adamantanone.

description of the virtual states, too. It has been claimed that this functional is the best choice for studying the noncovalent interactions, and it represents the most accurate generalized gradient approximation until now.

All these novel findings regarding both absolute and relative chemical shift values further support the statement of Bühl et al., according to which "a DFT route to NMR spectra" is already open.[38]

5. CONCLUSIONS

Theoretical ^{13}C and ^{1}H chemical shift values (with respect to TMS) and the relative shifts (with respect to the most deshielded center in the molecule) are reported for three cagelike systems: adamantane, 2-adamantanone, and 2,4-methano-2,4-dehydroadamantane. The mentioned parameters were computed at HF, BLYP, and B3LYP/6-311+G(2*d*,*p*) levels of theory, for the BLYP and B3LYP/6-31G(d,p) optimized geometries of the mentioned compounds, employing the CSGT and GIAO algorithms for achievement of gauge invariance. Except for the inverted carbon atoms and some of their nearest neighbors, the computed chemical shifts (with respect to TMS) at the HF level of theory showed significantly better agreement with the experimental data than the DFT values, which are systematically too deshielded. The last finding may be attributed to the inappropriate description of paramagnetic contribution to the shielding

tensor within the Kohn−Sham approach. On the contrary, the *relative shielding* values (with respect to the most deshielded center within the molecule) computed at DFT levels are significantly superior over the HF ones. It thus seems that although inferior to both HF and other correlated methods on an absolute scale, DFT methods may be successfully applied when the relative shieldings within the molecular system are of interest. For a given algorithm for achievement of gauge invariance, the correlation of calculated relative shift values with the experimental data are *systematically* significantly better at DFT than at HF level of theory. Among all of the employed DFT methods, the MPW1PW91 performs best from all aspects, due to its significantly improved long-range behavior (and thus much better description of virtual electronic states).

REFERENCES AND NOTES

(1) Olah, G. A.; Shamma, T.; Burrichter, A.; Rasul, G.; Prakash, G. K. S. *J. Am. Chem. Soc.* **1997**, *119*, 12923−12928.
(2) Wiberg, K. B.; McMurdie, N. *J. Am. Chem. Soc.* **1994**, *116*, 11990−11998.
(3) Haw, J. F.; Nicholas, J. B.; Xu, T.; Beck, L. W.; Ferguson, D. B. *Acc. Chem. Res.* **1996**, *29*, 259−267.
(4) A. de Dios, C.; Pearson, J. G.; Oldfield, E. *Science* **1993**, *260*, 1491−1496.
(5) Copie, V.; Battles, J. A.; Schwab, J. M.; Torchia, D. A. *J. Biomol. NMR* **1996**, *7*, 335−340.
(6) K. MacKenzie, R.; Prestegard, J. H.; Engelman, D. M. *J. Biomol. NMR* **1996**, *7*, 256−260.
(7) Dykstra, C. E. *Quantum Chemistry & Molecular Spectroscopy*; Prentice Hall, NJ, 1992; pp 336−347.
(8) Cheeseman, J. R.; Trucks, G. W.; Keith, T. A.; Frisch, M. J. *J. Chem. Phys.* **1996**, *104*, 5497−5509.
(9) Webb, G. A. In *Nuclear Magnetic Shieldings and Molecular Structure*; Tossell, J. A., Ed.; Kluwer Publishers: Netherlands, 1993; pp 1−25.
(10) Ditchfield, R. *Mol. Phys.* **1974**, *27*, 789−807.
(11) Wolinski, K.; Hinton, J. F.; Pulay, P. *J. Am. Chem. Soc.* **1990**, *112*, 8251−8260.
(12) Pulay, P.; Hinton, J. F.; Wolinski, K. In *Nuclear Magnetic Shieldings and Molecular Structure*; Tossell, J. A., Ed.; Kluwer Publishers: Netherlands, 1993; pp 243−262.
(13) Keith, T. A.; Bader, R. F. W. *Chem. Phys. Lett.* **1992**, *194*, 1−8.
(14) Keith, T. A.; Bader, R. F. W. *Chem. Phys. Lett.* **1993**, *210*, 223−231.
(15) Keith, T. A.; Bader, R. F. W. *J. Chem. Phys.* **1993**, *99*, 3669−3682.
(16) Rablen, P. R.; Pearlman, S. A.; Finkibiner, J. *J. Phys. Chem. A* **1999**, *103*, 7357−7363.
(17) Sitkoff, D.; Case, D. A. *J. Am. Chem. Soc.* **1997**, *119*, 12262−12273.
(18) Olah, G. A.; Burrichter, A.; Rasul, G.; Christe, K. O.; Surya Prakash, G. K. *J. Am. Chem. Soc.* **1997**, *119*, 4345−4352.
(19) Hinton, J. F.; Guthrie, P. L.; Pulay, P.; Wolinski, K.; Fogarasi, G. *J. Magn. Reson.* **1992**, *96*, 154−158.
(20) McMichael Rohlfing, C.; Allen, L. C.; Ditchfield, R. *J. Chem. Phys.* **1983**, *79*, 4958−4966.
(21) Schindler, M. *J. Am. Chem. Soc.* **1987**, *109*, 1020−1033.
(22) Kutzelnigg, W.; van Wullen, Ch.; Fleischer, U.; Franke, R.; Mourik, T. v. In *Nuclear Magnetic Shieldings and Molecular Structure*; Tossell, J. A., Ed.; Kluwer Publishers: Netherlands, 1993; pp 141−161.
(23) Hansen, A. E.; Bouman, T. D. In *Nuclear Magnetic Shieldings and Molecular Structure*; Tossell, J. A., Ed.; Kluwer Publishers: Netherlands, 1993; pp 117−140.
(24) Kutzelnigg, W. *Isr. J. Chem.* **1980**, *19*, 193−200.
(25) Schleyer, P. v. R.; de M. Carneiro, J. W.; Koch, W.; Forsyth, D. A. *J. Am. Chem. Soc.* **1991**, *113*, 3990−3992.
(26) Jameson, C. J.; de Rios, A. C. In *Nuclear Magnetic Shieldings and Molecular Structure*; Tossell, J. A., Ed.; Kluwer Publishers: Netherlands, 1993; pp 95−116.
(27) Jameson, C. J.; de Rios, A. C. *J. Chem. Phys.* **1992**, *97*, 417−434.
(28) Bak, K. L.; Hansen, A. E.; Stephens, P. J. *J. Phys. Chem.* **1995**, *99*, 17359−17363.
(29) Fukui, H.; Baba, T.; Matsuda, H.; Miura, K. *J. Chem. Phys.* **1994**, *100*, 6608−6613.
(30) Tossell, J. A. *Chem. Phys. Lett.* **1999**, *303*, 435−440.
(31) Cmoch, P.; Wiench, J. W.; Stefaniak, L.; Webb, G. A. *Spectrochim. Acta A* **1999**, *55*, 2207−2214.
(32) Orendt, A. M.; Facelli, J. C.; Grant, D. M. *Chem. Phys. Lett.* **1999**, *302*, 499−504.
(33) Kintop, J. A.; Machado, W. V. M.; Franco, M.; Toma, H. E. *Chem. Phys. Lett.* **1999**, *309*, 90−94.
(34) Galasso, V. *Chem. Phys.* **1999**, *241*, 247−255.
(35) Pecul, M.; Sadlej, J. *Chem. Phys.* **1998**, *234*, 111−119.
(36) Wilson, P. J.; Amos, R. D.; Handy, N. C. *Mol. Phys.* **1999**, *97*, 757−768.
(37) Wiberg, K. B. *J. Comput. Chem.* **1999**, *20*, 1299−1303.
(38) Buhl, M.; Kaupp, M.; Malkina, O. L.; Malkin, V. G. *J. Comput. Chem.* **1999**, *20*, 91−105.
(39) Borowski, P.; Janowski, T.; Wolinski, K. *Mol. Phys.* **2000**, *98*, 1331−1341.
(40) Gauss, J. *J. Chem. Phys.* **1993**, *99*, 3629−3643.
(41) Astrand, P.; Mikhelsen, K. V. *J. Chem. Phys.* **1996**, *104*, 648−653.
(42) van Wullen, Ch.; Kutzelnigg, W. *J. Chem. Phys.* **1996**, *104*, 2330−2340.
(43) Perera, S. A.; Nooijen, M.; Bartlett, R. J. *J. Chem. Phys.* **1996**, *104*, 3290−3305.
(44) Parr, R. G.; Yang, W. *Density Functional Theory of Atoms and Molecules*; Oxford University Press: Oxford, 1989.
(45) Seminario, J. M. An Introduction to Density Functional Theory in Chemistry. In *Modern Density Functional Theory*; Seminario, J. M., Politzer, P., Ed.; Elsevier Science B. V.: 1995; pp 1−27.
(46) Hohenberg, P.; Kohn, W. *Phys. Rev. B* **1964**, *136*, 864−871.
(47) Kohn, W.; Sham, L. J. *Phys. Rev. A* **1965**, *140*, 1133−1138.
(48) Becke, A. D. *Phys. Rev. A* **1988**, *38*, 3098−3100.
(49) Vosko, S. H.; Wilk, L.; Nusair, M. *Can. J. Phys.* **1980**, *58*, 1200−1211.
(50) Lee, C.; Yang, W.; Parr, R. G. *Phys. Rev. B* **1988**, *37*, 785−789.
(51) Perdew, J. P. *Phys. Rev. B* **1986**, *33*, 8822−8824.
(52) Perdew, J. P.; Wang, Y. *Phys. Rev. B* **1992**, *45*, 13244-.
(53) Becke, A. D. *J. Chem. Phys.* **1993**, *98*, 5648−5652.
(54) Adamo, C.; Barone, V. *J. Chem. Phys.* **1998**, *108*, 664−675.
(55) Scott, A. P.; Radom, L. *J. Phys. Chem.* **1996**, *100*, 16502−16513.
(56) Pejov, Lj.; Stefov, V. Šoptrajanov, B. *Vibr. Spectrosc.* **1999**, *19*, 435−439.
(57) Esposti, A. D.; Zerbetto, F. *J. Phys. Chem. A* **1997**, *101*, 7283−7291.
(58) Pejov, Lj. *Chem. Phys. Lett.* **2001**, *339*, 269−278.
(59) Vikić-Topić, D.; Pejov, Lj. *Croat. Chem. Acta* **2000**, *73*, 1057−1075.
(60) Vikić-Topić, D.; Pejov, Lj. *Croat. Chem. Acta* **2001**, *74*, 277−293.
(61) Bistričić, L.; Baranović, G.; Šafar-Cvitaš, D.; Mlinarić-Majerski, K. *J. Phys. Chem. A* **1997**, *101*, 941−952.
(62) Majerski, Z.; Mlinarić-Majerski, K.; Meić, Z. *Tetrahedron Lett.* **1980**, *21*, 4117−4118.
(63) Schlegel, H. B. *J. Comput. Chem.* **1982**, *3*, 214−218.
(64) Baranović, G.; Bistričić, L.; Pejov, Lj. Manuscript in preparation.
(65) Gaussian 98 (Revision A.9); Frisch, M. J.; Trucks, G. W.; Schlegel, H. B.; Scuseria, G. E.; Robb, M. A.; Cheeseman, J. R.; Zakrzewski, V. G.; Montgomery, J. A.; Stratmann, R. E.; Burant, J. C.; Dapprich, S.; Millam, J. M.; Daniels, A. D.; Kudin, K. N.; Strain, M. C.; Farkas, O.; Tomasi, J.; Barone, V.; Cossi, M.; Cammi, R.; Mennucci, B.; Pomelli, C.; Adamo, C.; Clifford, S.; Ochterski, J.; Petersson, G. A.; Ayala, P. Y.; Cui, Q.; Morokuma, K.; Malick, D. K.; Rabuck, A. D.; Raghavachari, K.; Foresman, J. B.; Cioslowski, J.; Ortiz, J. V.; Stefanov, B. B.; Liu, G.; Liashenko, A.; Piskorz, P.; Komaromi, I.; Gomperts, R.; Martin, R. L.; Fox, D. J.; Keith, T.; Al-Laham, M. A.; Peng, C. Y.; Nanayakkara, A.; Gonzalez, C.; Challacombe, M.; Gill, P. M. W.; Johnson, B. G.; Chen, W.; Wong, M. W.; Andres, J. L.; Head-Gordon, M.; Replogle, E. S.; Pople, J. A. Gaussian, Inc.: Pittsburgh, PA, 1998.
(66) Majerski, Z.; Vinković, V.; Meić, Z. *Org. Magn. Res.* **1981**, *17*, 169−171.
(67) Vikić-Topić, D.; Pejov, Lj. In *Book of Abstracts of The 3rd International Dubrovnik NMR Course and Conference*; Vikić-Topić, D., Ed.; Croatia, 2000; pp 49−49 (ISBN 953-6690-10-1).
(68) Jameson, A. K.; Jameson, C. J. *Chem. Phys. Lett.* **1987**, *134*, 461−466.

CI010042M